

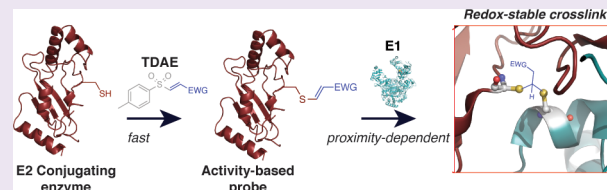
Orthogonal Thiol Functionalization at a Single Atomic Center for Profiling Transthiolation Activity of E1 Activating Enzymes

Mathew Stanley, Cong Han, Axel Knebel, Paul Murphy, Natalia Shpiro, and Satpal Virdee*

MRC Protein Phosphorylation and Ubiquitylation Unit, College of Life Sciences, University of Dundee, Dow Street, Dundee DD1 SEH, United Kingdom

S Supporting Information

ABSTRACT: Transthiolation is a fundamental biological reaction and is utilized by many enzymes involved in the conjugation of ubiquitin and ubiquitin-like proteins. However, tools that enable selective profiling of this activity are lacking. Transthiolation requires cysteine–cysteine juxtaposition; therefore a method that enables irreversible “stapling” of proximal thiols would facilitate the development of novel probes that could be used to profile this activity. Herein, we characterize biocompatible chemistry that enables sequential functionalization of cysteines within proteins at a single atomic center. We use our method to develop a new class of activity-based probe that profiles transthiolation activity of human E1 activating enzymes. We demonstrate use *in vitro* and *in situ* and compatibility with competitive activity-based protein profiling. We also use the probe to gain insight into the determinants of transthiolation between E2 and a RING-in-between-RING (RBR) E3 ligase. Furthermore, we anticipate that this method of thiol functionalization will have broad utility by enabling simple redox-stable cross-linking of proximal cysteines in general.



Post-translational modification of substrate proteins with ubiquitin (Ub) and ubiquitin-like proteins (Ubls) regulates almost all aspects of eukaryotic biology, and alterations in Ub/Ubl conjugation pathways are associated with a growing number of pathologies.¹ Conjugation of Ub to substrates typically targets them for degradation by the proteasome,² a megadalton protease, and proteasome inhibition is an approved mode of therapy for the treatment of multiple myeloma with excellent success rates.³ Conjugation of Ubls, of which there are approximately 20 in humans,⁴ have specialized cellular roles, and an inhibitor that selectively blocks conjugation of the Ubl NEDD8 is in clinical development for the treatment of cancer.⁵

Ub/Ubl conjugation is orchestrated by an enzymatic cascade consisting of E1 activating enzymes (E1s), E2 conjugating enzymes (E2s), and E3 ligases (E3s).² To ensure fidelity in conjugation, Ub/Ubls have their own cognate but homologous machinery.⁶ Ub/Ubl conjugation begins with E1-catalyzed activation of the C-terminus of the Ub/Ubl. Attack of the activated Ub/Ubl by an E1 catalytic cysteine forms a labile thioester conjugate between E1 and Ub/Ubl (E1~Ub/Ubl).^{7,8} Next, E2 binding results in juxtaposition of cysteine residues in E1 and E2 that mediates transthiolation of Ub/Ubl, resulting in formation of a thioester conjugate between E2 and Ub/Ubl (E2~Ub/Ubl).⁹ Finally, transfer of Ub/Ubl to *ε*-amino groups of lysine residues within specific substrates is mediated by E3s.^{10–12} E3s belonging to the HECT and RBR subfamilies also undergo transthiolation with E2 ~ Ub, forming a thioester conjugate between E3 and Ub.¹³ The Ub conjugation machinery consists of ~35 cognate E2s which can dictate the topology, site, and extent of substrate ubiquitination.¹⁴ All of these factors influence the biological outcome of the

modification. On the other hand, the Ubl conjugation machineries typically have a single cognate E2.⁴ Therefore, inhibition of E1–E2 transthiolation activity is an attractive strategy for selectively modulating or ablating Ub/Ubl conjugation.¹⁵

The enzymatic cascade associated with Ub/Ubl conjugation makes the development of inhibitors, or activators, challenging. Tools that selectivity monitor discrete steps in Ub/Ubl conjugation, particularly transthiolation, are needed to fully realize the therapeutic potential of Ub/Ubl systems in an efficient manner. Furthermore, such tools could be used to further our limited understanding of the biological regulatory mechanisms associated with E1–E2 activities.^{16,17} There has also been a long-standing interest in the specificity and conformational determinants associated with E1–E2 activity.^{18–21} Tools that allow formation of stabilized versions of the transient E1–E2 transthiolation intermediates would undoubtedly facilitate their structure determination. Importantly, the stabilized versions should accurately mirror the geometry of the native intermediate so that mechanistically relevant insight can be garnered.

Activity-based probes (ABPs) have proven to be powerful tools that enable profiling of a discrete enzymatic activity without protein purification or substrate identification; a platform known as activity-based protein profiling (ABPP).^{22,23} They can also be used in complex proteomes,

Received: November 11, 2014

Accepted: April 6, 2015

Published: April 6, 2015



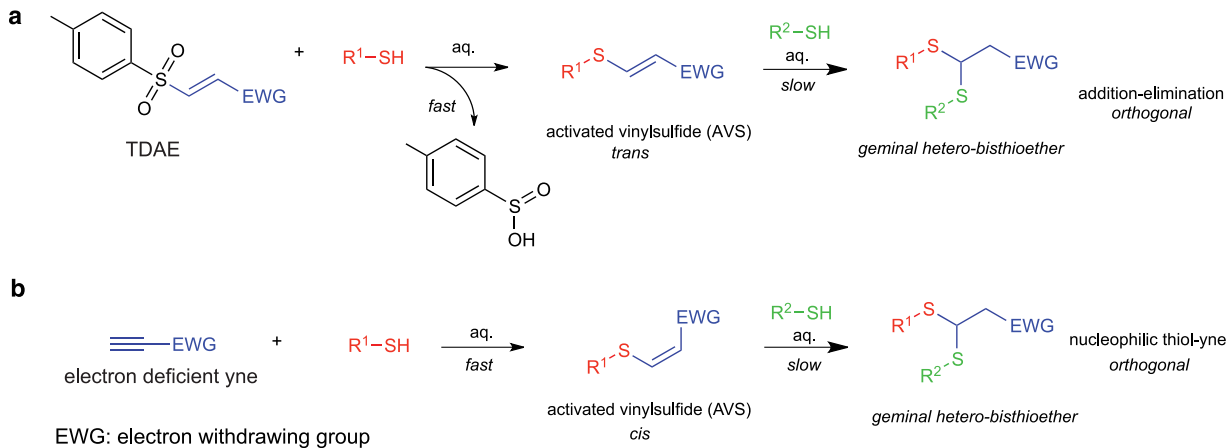


Figure 1. Prospective chemistry for biocompatible orthogonal thiol functionalization (OTF). (a) Reaction of a tosyl-substituted doubly activated ene (TDAE) with a thiol affords the *trans* activated vinylsulfide (AVS). The installed AVS could serve as a warhead that covalently reacts with a proximal cysteine. Addition of a second thiol to the AVS is much slower, thereby enabling OTF. Reactivity of the AVS should be tunable by altering the strength of the EWG in the TDAE. (b) Alternatively, nucleophilic thiol-yne addition to an electron-deficient yne can yield a *cis* AVS. Addition of a second thiol to the AVS can commence and may have different kinetics compared to a *trans* AVS due to steric and electronic effects.

and in competitive mode. Because a prerequisite for trans-thiolation activity is cysteine–cysteine juxtaposition, we reasoned that a tagged E2 enzyme with a thiol-reactive warhead installed on its catalytic cysteine could be used as an ABP to profile E1–E2 transthioleation activity. E2s are >17 kDa, and the catalytic cysteine resides within the middle of the polypeptide.¹⁴ Therefore, a desirable strategy would be to treat recombinant reporter-tagged E2 with a molecule that installs a warhead with a small steric footprint that can then react with a second cysteine in an orthogonal manner. The second reaction should only occur under proximity-accelerated conditions arising from native E1–E2 activity and be compatible with complex cell extracts where cellular thiols such as glutathione are abundant. To accurately mirror the tetrahedral and transient trans-thiolation intermediate,²⁴ and to ensure native activities are captured, functionalization at a single atomic center would be an important feature. Despite there being a rich repertoire of biocompatible cysteine chemistry,^{25,26} there is a paucity of reactions that achieve this. One strategy for achieving the required orthogonal thiol functionalization (OTF) would be to use a molecule that can be bifunctionalized with thiols where the first step is chemoselective and quantitative, but where the second step is much slower. Additionally, the chemistry should be redox-stable and compatible with micromolar protein concentrations, an aqueous buffer and near-physiological pH and temperature.

RESULTS AND DISCUSSION

Novel Biocompatible Chemistry for Orthogonal Thiol Functionalization.

Radical thiol-yne chemistry has been used to carry out sequential thiol functionalization in protein contexts.^{27,28} However, functionalization occurs at two distinct atomic centers, and the requisite UV exposure and radical chemistry can result in side reactions that would be exacerbated in complex biological samples.^{29,30} In light of the absence of biocompatible chemistry for sequential functionalization at a single atomic center, we were attracted to two classes of nucleophilic (i.e., radical-free) thiol addition reactions to either doubly activated (electron deficient) enes or activated ynes that yield an activated vinylsulfide (AVS). An AVS could potentially serve as a novel thiol-reactive warhead and covalently label

proximal cysteine residues yielding a stable and tetrahedral, geminal heterobisthioether. The first class of reaction involves thiol addition to a phenylsulfonyl substituted- or a tosyl substituted-doubly activated ene (TDAE)^{31,32} which in aqueous buffer yields the *trans* AVS via an unexpected addition–elimination mechanism³² (Figure 1a). The second class of reaction involves nucleophilic thiol-yne addition to activated ynes,^{33–35} which in aqueous buffer yields the *cis* AVS³⁵ (Figure 1b). Studies of the reactivity of a thiol toward the AVS produced by nucleophilic thiol-yne have been carried out, and the OTF of activated ynes in organic solvent has been demonstrated with small molecule thiols.^{35,36} To explore this chemistry further, we initially carried out reactions between a model protein and peptide to evaluate biocompatibility, stability, and chemoselectivity. We also carried out kinetic measurements of the second functionalization step to ascertain if they were consistent with restricted labeling of proximal cysteines.

Model Reactions for Installing an Activated Vinylsulfide (AVS). As a model protein to test novel methods for thiol functionalization in protein contexts, we prepared a truncated form of Ub missing its C-terminal Gly–Gly residues (ΔUb). To ΔUb , a C-terminal thiol group was appended using a semisynthetic strategy which yielded $\Delta\text{Ub-SH}$ (Figure 2a; Supporting Figure S1A).^{22,23} The rationale for such a species was several-fold: (i) Ub does not contain any native cysteines. (ii) Ub generates a consistent and clean electrospray ionization (ESI) mass spectrum allowing unambiguous assignment of protein adducts. (iii) $\Delta\text{Ub-SH}$ functionalized with an AVS should have ABP activity allowing assessment of the proximity dependence of the second cysteine functionalization step in a biological context. To clarify the latter point, after successful thiol functionalization of $\Delta\text{Ub-SH}$ to form an AVS, the truncation would result in the reactive center being nearly spatially equivalent to the C-terminal carbonyl carbon atom of full-length Ub (Supporting Figure S1B and C). Enzymes that hydrolyze the C-terminus of ubiquitin from substrates (DUBs) form an acyl-Cys intermediate with the terminal Ub carbonyl.³⁷ Therefore, AVS functionalized $\Delta\text{Ub-SH}$ would be expected to function as an ABP and covalently label active DUBs in a proximity-dependent reaction like related ABPs.³⁸

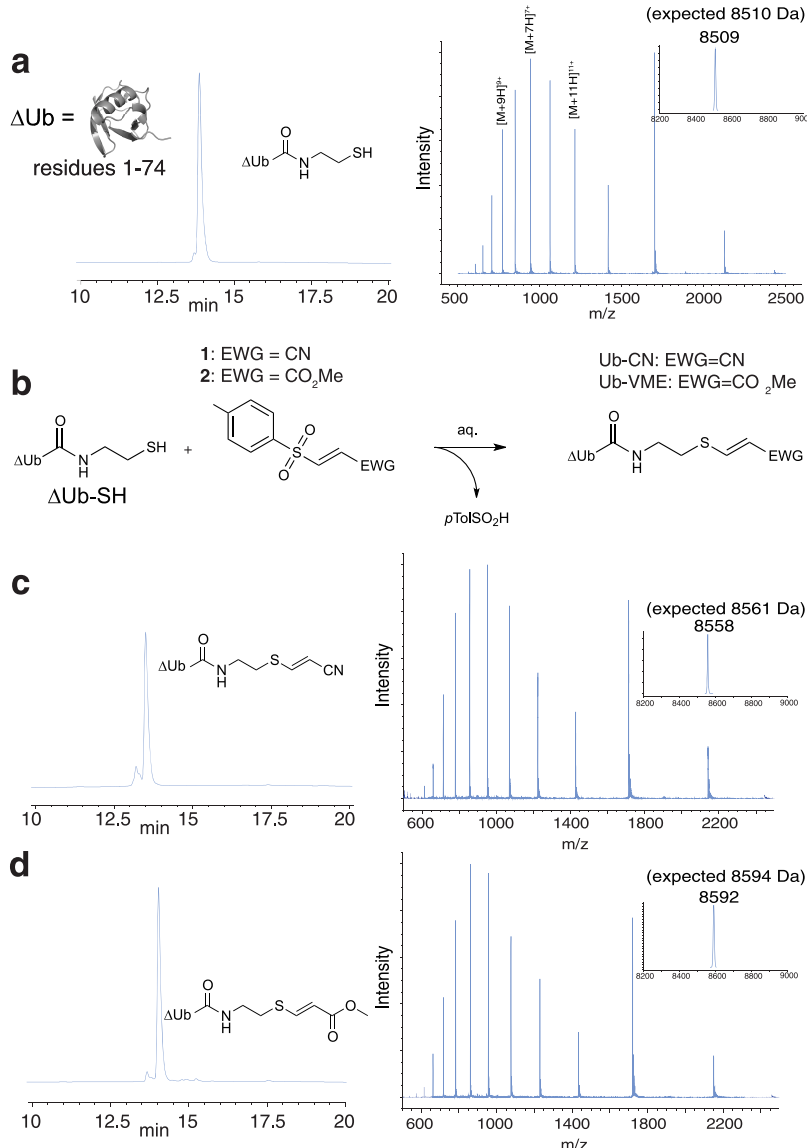


Figure 2. Model reactions for installing AVS warheads by thiol labeling. (a) $\Delta\text{Ub-SH}$ was prepared using a semisynthetic strategy and characterized by LC-MS. Left, HPLC chromatogram of $\Delta\text{Ub-SH}$ (214 nm). Right, electrospray ionization-mass spectrometry (ESI-MS) spectra of $\Delta\text{Ub-SH}$ (found, 8509 Da; expected, 8510 Da). (b) Reaction schematic depicting an addition–elimination reaction between $\Delta\text{Ub-SH}$ and a tosyl-substituted doubly activated ene (TDAE). The thiol in $\Delta\text{Ub-SH}$ is converted to an activated vinylsulfide (AVS). The elimination product is the innocuous sulfinic acid. (c) LC-MS analysis of the thioacrylonitrile AVS product, $\Delta\text{Ub-CN}$, after reaction of $\Delta\text{Ub-SH}$ with 4 equiv of **1** in pH 8 aqueous phosphate buffer. Reaction was incubated at 37 °C for 1 h. Left, HPLC chromatogram of $\Delta\text{Ub-CN}$ (214 nm). Right, ESI-MS spectra of $\Delta\text{Ub-CN}$ (found, 8558 Da; expected, 8561 Da). (d) LC-MS analysis of the thiomethyl acrylate AVS product, $\Delta\text{Ub-VME}$, after reaction of $\Delta\text{Ub-SH}$ with 4 equiv of **2** in pH 8 aqueous phosphate buffer. Reaction was incubated at 37 °C for 1 h. Left, HPLC chromatogram of $\Delta\text{Ub-VME}$ (214 nm). Right, electrospray ionization-mass spectrometry (ESI-MS) spectra of $\Delta\text{Ub-VME}$ (found, 8592 Da; expected, 8594 Da).

Δ Ub-SH was purified by preparative reversed phase high-performance liquid chromatography (RP-HPLC) and folded in pH 8.0 phosphate buffer and characterized by liquid chromatography–mass spectrometry (LC-MS; Figure 2a). TDAE compounds were then tested for their ability to label the thiol group on Δ Ub-SH with an AVS (Figure 2b). At a protein concentration of 1 mg mL⁻¹ (120 μ M), the addition of 4 equiv of TDAE 1 resulted in quantitative modification of Δ Ub-SH within 1 min at 37 °C as determined by LC-MS (Supporting Figure S2). LC-MS analysis confirmed that the product was the thioacrylonitrile AVS (Δ Ub-CN; Figure 2c). No bifunctionalization with Δ Ub-SH was observed and neither was modification of Ub without a thiol group (data not shown). We next tested the generality of the addition–elimination

mechanism for installing a *trans* AVS by exploring a TDAE with a different electron withdrawing group (EWG). If the addition–elimination mechanism was conserved, then this would provide a means to tune the reactivity of the AVS simply by altering the strength of the electron withdrawing group in the TDAE. We chose TDAE **2**, which contains a methyl acrylate group, and synthesized it as previously described (Supporting Figure S3 and Methods).³⁹ Labeling with **2** could be readily carried out under the same conditions employed for **1** and afforded a product with a mass consistent with the corresponding thiomethyl acrylate AVS ($\Delta\text{Ub-VME}$; Figure 2d). Similarly to **1**, no bifunctionalization with $\Delta\text{Ub-SH}$ was observed. This demonstrated that facile, rapid, and chemoselective thiol labeling with TDAEs **1** and **2** produced $\Delta\text{Ub-SH}$.

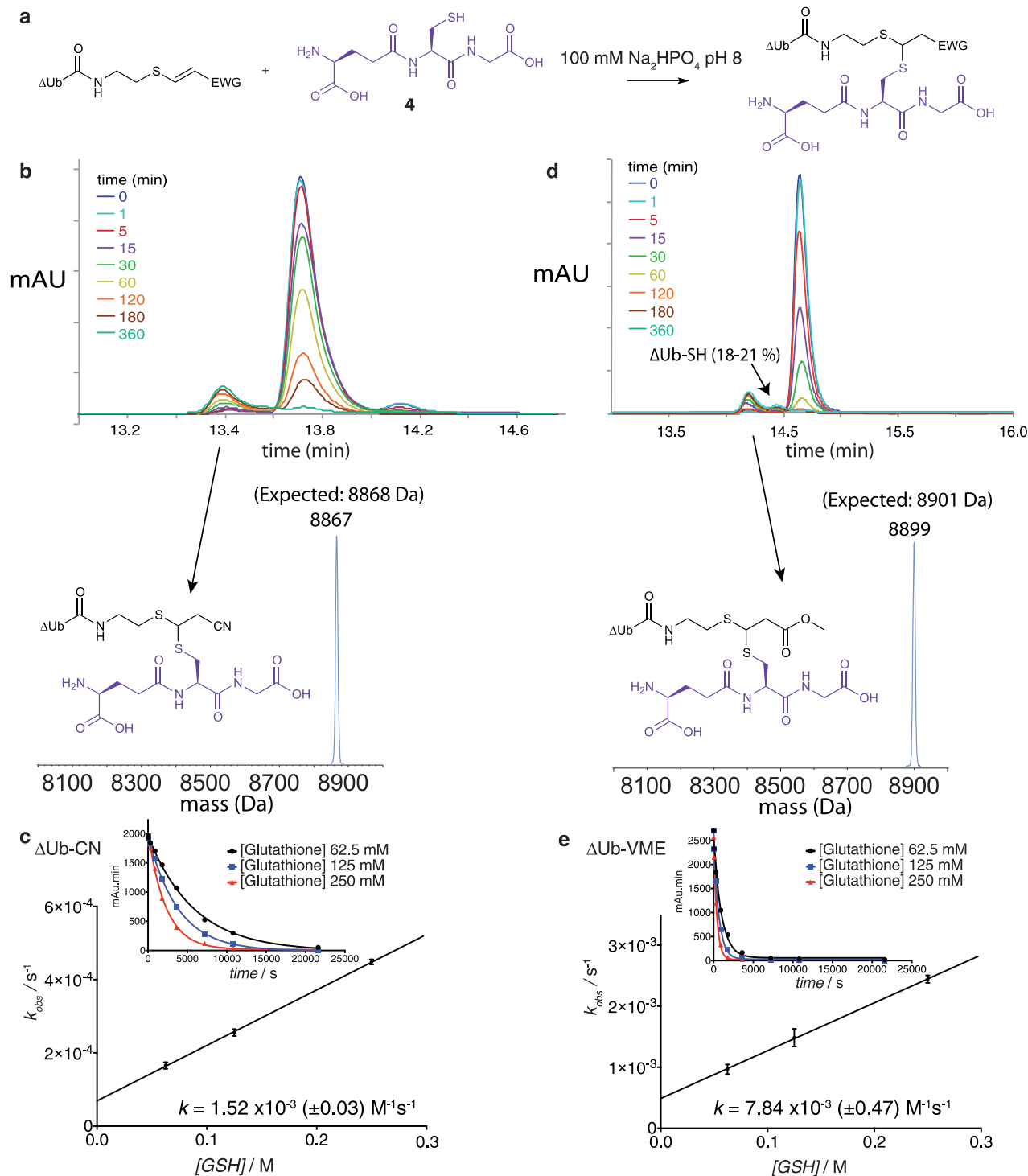


Figure 3. Kinetics of cysteine addition to AVS warheads, which can be modulated and are consistent with proximity dependence. (a) Schematic for reaction of $\Delta\text{Ub-SH}$ bearing an AVS with **4**. Reactions were carried out in pH 8 phosphate buffer at 37°C . (b) Representative reaction between $\Delta\text{Ub-CN}$ ($30 \mu\text{M}$) and **4** (62.5 mM). Reaction was monitored by LC-MS analysis of acid quenched samples at various time points. Reaction was complete after 360 min. The product was the addition adduct with **4** (found, 8867; expected, 8868 Da). AVS starting material ($t_R = 13.7 \text{ min}$) has a considerably higher extinction coefficient at 280 nm compared to the heterobisthioether product ($t_R = 13.4 \text{ min}$). (c) Determination of the second order rate constant under pseudo-first-order conditions for the reaction between **4** and $\Delta\text{Ub-CN}$. Integrated peak values at three different concentrations of **4** were plotted against time and fitted to a single exponential function. The half-life was determined and used to deduce the observed rate constant, which was plotted against the concentration of **4**. The second order rate constant was determined from the slope. Error bars represent $\pm \text{s.d.}$ from two independent reactions at each concentration. (d) Representative reaction between $\Delta\text{Ub-VME}$ ($30 \mu\text{M}$) and **4** (62.5 mM). The product was the addition adduct with **4** (found, 8899; expected, 8901 Da). Reaction was complete after 180 min. AVS starting material, $t_R = 14.65 \text{ min}$; heterobisthioether product, $t_R = 14.2 \text{ min}$. Some elimination of $\Delta\text{Ub-SH}$ is observed ($t_R = 14.45 \text{ min}$). (e) Determination of the second order rate constant under pseudo-first-order conditions for the addition of **4** to $\Delta\text{Ub-VME}$. The experiment was carried out as described for $\Delta\text{Ub-CN}$.

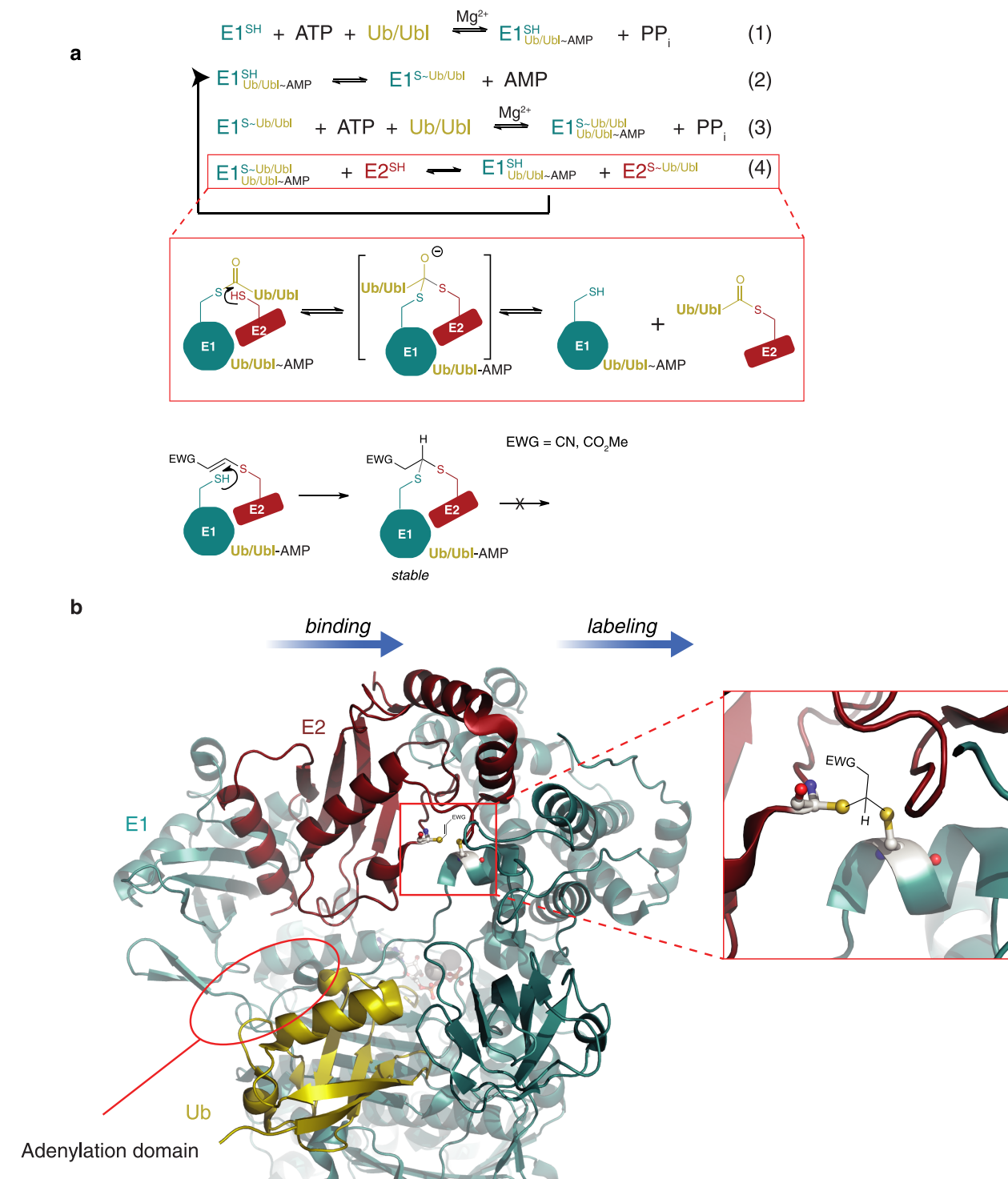


Figure 4. Strategy for building a new class of activity-based probe for profiling transthiolation activity. (a) Catalytic cycle of E1s (superscripts correspond to covalent modifications of the E1 catalytic cysteine, subscripts correspond to noncovalent association of Ub/Ubl species with the adenylation domain and “~” corresponds to a labile bond). Initially, the E1 adenylation domain catalyzes the C-terminal adenylation of Ub/Ubl (step 1). Subsequent attack of the E1 catalytic cysteine leads to thioesterification of the E1 with Ub/Ubl (E1~Ub/Ubl; step 2). E1~Ub/Ubl can noncovalently bind a second Ub/Ubl and catalyze its adenylation (step 3). Next, E1 recruits E2, resulting in cysteine–cysteine juxtaposition, which leads to transthiolation and formation of E2~Ub/Ubl (step 4). Step 4 is also depicted in cartoon format. (b) Strategy for building a novel probe for profiling E1–E2 transthiolation activity by installing an AVS on the catalytic cysteine of recombinantly expressed and purified E2. The cysteine–cysteine juxtaposition that occurs between a functional E1–E2 pair is exploited. Incubation with an active and cognate E1 would recruit the E2 ABP, and proximity-dependent covalent cross-linking would occur. The heterobisthioether cross-link would have similar tetrahedral geometry to the transient transthiolation intermediate. Unlike the enzyme intermediate, the cross-linked species is stable. The figure is a model, and we cannot formally exclude that the actual cross-linked complex may be structurally different. Model based on PDB ID 4II2.²⁰

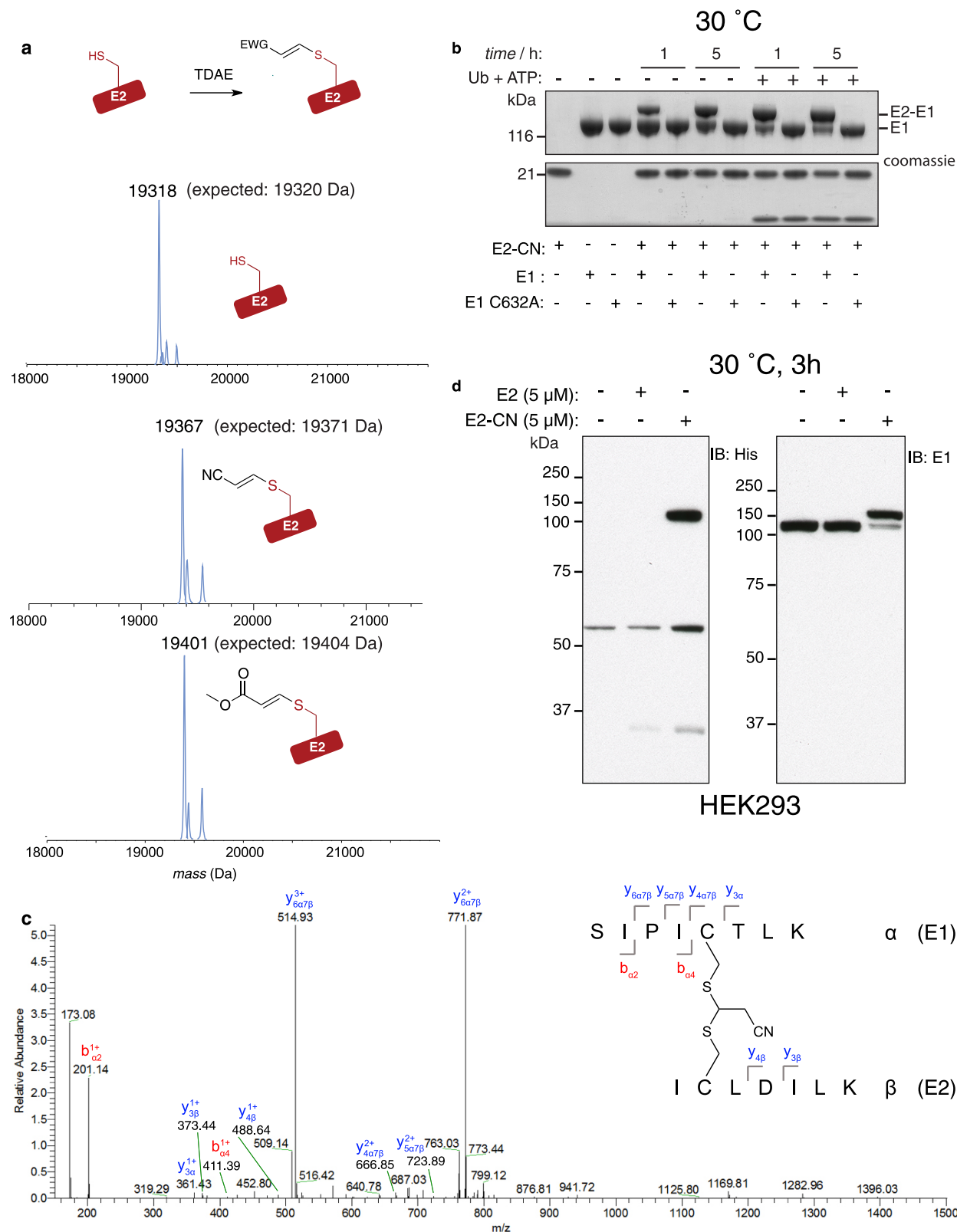


Figure 5. Activity-based protein profiling of E1 enzyme transthiolation activity. (a) Deconvoluted ESI-MS spectrum for unmodified, Ni-NTA purified UBE2N (top; found, 19318 Da; expected, 19320 Da). Deconvoluted ESI-MS spectrum for thioacrylonitrile-functionalized E2, UBE2N-CN (middle; major product, found, 19367 Da; expected, 19371 Da). Deconvoluted ESI-MS spectrum for thiomethyl acrylate-functionalized E2, UBE2N-VME (bottom; major product, found, 19401 Da; expected, 19404 Da). UBE2N was functionalized with the AVS by incubation with 4 equiv of 1 or 2 and incubated at 37 °C for 1 h in pH 8 phosphate buffer. (b) Incubation of E2-CN (UBE2N-CN; 3 μM) with recombinant UBA1 (12 μM) results in efficient, time-dependent labeling (lanes 4 and 6), which is enhanced in the presence of Ub and ATP (lanes 8 and 10 vs 4 and 6). No labeling is observed in UBA1 C632A despite it containing 18 cysteine residues (lanes 5, 7, 9, and 11). Proteins were resolved by SDS-PAGE followed by coomassie staining. (c) Annotated tryptic MS/MS spectrum for a triply charged precursor ion (observed m/z = 581.3360; expected m/z =

Figure 5. continued

581.3371). Theoretical m/z 's for the most intense $y^{2+}_{\alpha\gamma\beta}$ and $y^{3+}_{\alpha\gamma\beta}$ ions are 771.99 (found, 771.87) and 515.00 (found, 514.93), respectively. Abundance axis has been scaled to 5% of the most intense ion ($m/z = 771.87$) so weaker signals are apparent. (d) Incubation of E2 (His-UBE2N) and E2-CN (His-UBE2N-CN) with HEK293 proteome obtained by detergent-based lysis. Left panel, ~140 kDa band is present when the AVS is installed on His-UBE2N (lane 3). The band is absent in the lysate-only control (lane 1) and when lysate is treated with His-UBE2N without an AVS warhead (lane 2). Right panel, Anti-UBA1 immunoblotting confirms the labeled protein is UBA1, which is ~90% labeled (lane 3). No UBA1 modification of lysate-only control (lane 1) or when lysate is treated with His-UBE2N without an AVS warhead (lane 2). Proteome was resolved by SDS-PAGE and transferred to nitrocellulose membrane and probed with anti-UBA1 antibody.

functionalized with two distinct AVSs. Modification of Δ Ub-SH with the electron deficient yne, methyl propiolate 3, under similar labeling conditions produced a species with a mass identical to that produced with 2. This was expected to be the *cis* variant of Δ Ub-VME (Δ Ub-VME*; Supporting Figure S4).

Model Orthogonal Functionalization. We next explored orthogonal functionalization with a second thiol. Small molecules were removed from functionalized Δ Ub-SH by buffer exchange, and as a model second thiol species we chose the tripeptide glutathione (GSH) 4. We carried out reactions in a reducing pH 8 phosphate buffer containing 0.1 mM tricarboxyethylphosphine (TCEP) at 37 °C (Figure 3a). We found that when a large excess of 4 (~2000 equiv) was added to Δ Ub-CN (30 μ M), after 60 min ~50% had been converted to a product with a mass consistent with the addition of 4 (Figure 3b). To determine if the rate of this reaction was suitable for proximity-dependent reactions, we determined the second order rate constant, k_2 , under pseudo-first-order conditions. This was achieved by an RP-HPLC assay (Figure 3c). For Δ Ub-CN, we found this to be $1.52 \times 10^{-3} (\pm 0.03)$ M $^{-1}$ s $^{-1}$. This value indicated that at low micromolar reactant concentrations, negligible addition of the second thiol would occur without proximity dependence as it would take >4 years to achieve 50% conversion with reactants at 5 μ M ($t = 1/k[\text{reactant}]_{t=0}$). We next studied the addition of 4 to Ub-VME (*trans*). This reaction also afforded a product with a mass consistent with the addition of 4 (Figure 3d). For this reaction, k_2 was $7.84 \times 10^{-3} (\pm 0.47)$ M $^{-1}$ s $^{-1}$ (Figure 3e). This was still consistent with proximity dependence at low micromolar reactant concentrations, but 5-fold higher than for Δ Ub-CN. This demonstrated that the reactivity of the AVS could be modulated within a modest kinetic window simply by altering the EWG substituent on the TDAE. However, formation of the adduct with 4 was accompanied by formation of some elimination product, Δ Ub-SH (18–21%; Figure 3d). After prolonged incubation for 45 h, further elimination was observed (~33%). We propose that this is due to the methyl ester substituent being a stronger EWG than the nitrile substituent that renders the β -hydrogen of the heterobisthioether more acidic. This promotes an elimination mechanism, which in this case regenerates Δ Ub-SH, albeit with slow kinetics ($t_{1/2} > 45$ h). This explains why when even stronger EWGs are present the heterobisthioether cannot be isolated.^{33,34} A similar phenomenon has been reported with geminal doubly activated vinyl compounds and has been exploited to prepare covalent yet reversible small molecule enzyme inhibitors.⁴⁰

To assess the reactivity of *trans* and *cis* regiosomers, observed rate constants for the addition of 4 to Δ Ub-VME (*trans*) and Δ Ub-VME* (*cis*) were determined. Δ Ub-VME* was found to be 5-fold slower than Ub-VME (1.7×10^{-4} s $^{-1}$ vs 8.8×10^{-4} s $^{-1}$) (Supporting Figure S5). This demonstrated that labeling with a TDAE affords a *trans* AVS which has greater

thiol reactivity, presumably on account of the steric and electronic affects associated with the different regiosomers. Similar levels of the elimination product were observed irrespective of the nature of the regiosomer.

To test whether Δ Ub-CN could act as an ABP toward DUBs like analogous species,³⁸ a panel of DUBs (5 μ M) was incubated with Δ Ub-CN (20 μ M) for 1 h at 30 °C. Of these, four out of six underwent detectable covalent labeling, presumably by specifically targeting the catalytic cysteine (Supporting Figure S6). OTUB2 was modified ~50% after 1 h, demonstrating that the reaction was accelerated by over 4 orders of magnitude relative to model reactions with 4. Taken together, these data illustrate that biocompatible, rapid, and chemoselective labeling of a protein thiol with an AVS can be carried out. The AVS is effectively inert at low micromolar concentrations, but proximity acceleration arising from native enzyme substrate interactions enhances the rate significantly, enabling efficient protein labeling in an activity-based manner.

Preparation of an Activity-Based Probes for Profiling Transthiolation.

The E1 catalytic cycle involves ATP-dependent adenylation of the C-terminus of the Ub/Ubl accompanied by a release of pyrophosphate (PP_i)⁸ (Figure 4a). Subsequent attack of Ub/Ubl-adenylate by an E1 catalytic cysteine forms a thioester conjugate between E1 and Ub (E1~Ub) accompanied by the release of adenosine monophosphate (AMP).⁸ Next, E2 binding results in juxtaposition of cysteine residues in E1 and E2 that mediates transthiolation of Ub/Ubl.^{9,20} We therefore reasoned that an E2 functionalized at its catalytic cysteine with an AVS would serve as a novel class of activity-based probe for profiling E1–E2 transthiolation activity by undergoing proximity-dependent covalent labeling of the catalytic cysteine in an active E1 (Figure 4b). We chose the Ub E2 UBE2N (~20 kDa) because it only contains a single cysteine and assembles nonproteasomal K63-linked polyubiquitin chains that regulate fundamental biological processes including immune signaling in response to cellular cytokines and pathogens and assembly of key repair complexes in response to DNA damage.^{41,42}

We expressed and purified UBE2N with an N-terminal hexahistidine tag (His-tag) (Supporting Figure S7 and Methods). Labeling with TDAEs 1, 2, and yne 3 could be carried out as described for Δ Ub-SH with predominant masses consistent with UBE2N functionalized with the corresponding thioacrylonitrile (UBE2N-CN) or thiomethyl acrylate AVSs (UBE2N-VME and UBE2N-VME*; Figure 5a, Supporting Figure S8).

Activity-based Protein Profiling of Recombinant E1 Activating Enzymes.

We next expressed and purified the wild type human ubiquitin E1 activating enzyme (UBA1) and a catalytically dead C632A mutant (Supporting Methods).⁴³ In pH 8 phosphate buffer, we incubated UBA1 (~120 kDa) or UBA1 C632A (3 μ M) with UBE2N-CN (12 μ M) at 30 °C. We observed time-dependent covalent modification of UBA1 as

detected by an electrophoretic shift on reducing sodium dodecyl sulfate-polyacrylamide gel electrophoresis (SDS-PAGE) analysis (Figure 5b). As it is known that a doubly loaded E1 stimulates E1–E2 transthiolation (Figure 4a, step 3),^{9,44} we also carried out labeling in the presence of Ub and ATP and observed significant enhancement in probe labeling ($\sim 75\%$ vs $\sim 25\%$ after 1 h). Taken together, these data showed that the probe underwent activity-based labeling of UBA1 and was sensitive enough to detect allosteric regulatory mechanisms that modulate E2 recruitment. In all cases, UBA1 C632A was not labeled, indicating that the 18 noncatalytic cysteine residues in UBA1 were not targeted. Formation of a heterobisthioether cross-link between UBE2N-CN and C632 in UBA1 was confirmed by tryptic MS/MS sequencing (Figure 5c). Similar labeling efficiency was observed with UBE2N-VME, suggesting that in this case, binding of the E2 probe to E1 or conformational changes were rate-limiting and not the kinetics of the second thiol addition step (Supporting Figure S9). Interestingly, labeling efficiency of UBA1 with UBE2N-VME* (*cis*) was significantly less efficient than with UBE2N-VME, emphasizing the value of the TDAE approach for installing an AVS (Supporting Figures S9 and S20). This was likely to be a reflection of the reduced kinetics we observed in model reactions of Δ Ub-VME* with 4, steric incompatibility with the *cis* AVS regioisomer, or a combination of both. Generality of the technology for profiling native transthiolation activity was evident from experiments carried out with E1s and E2s from the NEDD8, SUMO, and ISG15 conjugation systems (Supporting Figures S10–S12). Importantly, these data showed that all probes were specific for their cognate E1, consistent with the profiling of native activity.

To test if small molecule nucleophiles would compromise probe activity by competing for the AVS, we tested the compatibility of probe labeling of UBA1 with thiol- and phosphine-based reducing agents commonly used in biological buffers. Labeling was completely unaffected by the presence of at least 10 mM dithiothreitol (DTT), 2-mercaptoethanol (BME), and TCEP (Supporting Figure S13). The heterobisthioether cross-link was also acid and redox stable even in the presence of elevated concentrations of reducing agent (Supporting Figure S14).

We next tested commercial and literature strategies for cysteine–cysteine cross-linking to see if E1 labeling was a unique property of our AVS warheads. Using the same approach, we prepared E2 probes labeled with dichloroacetone, bismaleimidoethane, and dibromomaleimide,⁴⁵ although E2 functionalized with dichloroacetone was particularly unstable and prone to elimination (Supporting Figure S15). We also explored radical thiol-ene/yne chemistry by alkylating the E2 cysteine with allyl bromide and propargyl bromide.²⁸ With the exception of the propargylated E2 probe, all were capable of undergoing model addition/addition–elimination reactions with 4 (Supporting Figure S16). When incubated with E1 under identical conditions employed for AVS functionalized probes, we found that labeling was barely perceptible except for E2 treated with bismaleimidoethane (UBE2N-BMOE) (Supporting Figure S17). However, this was less efficient than AVS functionalized E2, and covalent labeling was perceptible in the C632A mutant sample, indicative of off-target labeling. Furthermore, this approach introduces an 8 Å extraneous linker and steric bulk between reactive cysteines (Supporting Figure S18). The second order rate constant for the addition of cysteine to the related *N*-ethylmaleimide is $\sim 1.5 \times 10^2 \text{ M}^{-1}$

s^{-1} .⁴⁶ As expected, the addition of 4 to prepared Δ Ub-BMOE was too rapid to assign a kinetic parameter under our assay conditions (Supporting Figure S19). These results illustrate that the sterics of our AVSs enable highly efficient and exquisitely specific profiling of transthiolation activity despite having rate constants orders of magnitude lower than conventional electrophiles.

In Situ Profiling of E1 Activating Enzyme (UBA1) in Complex Proteomes. We next tested if UBE2N-CN could efficiently label endogenous UBA1 without any off-target labeling in the context of a complex mammalian proteome. Incubation of UBE2N-CN (5 μM) with Human Embryonic Kidney 293 (HEK293) extract (2.8 mg mL⁻¹) for 3 h at 30 °C followed by immunoblotting against the N-terminal His-tag on UBE2N-CN resulted in a single clear band migrating at a molecular weight consistent with endogenous UBA1 modified with UBE2N (Figure 5d, lane 3, left panel; Supporting Figure S20). We confirmed that the labeled species was indeed UBA1 by immunoblotting with anti-UBA1 antibody, which indicated that labeling efficiency was >90% (Figure 5d, lane 3, right panel). The fact that no other labeled proteins were detected in the anti-His immunoblots demonstrated that UBE2N-CN and UBE2N-VME were exquisitely specific for UBA1. We also treated the extract with UBE2N-BMOE (Supporting Figure S21). Numerous additional bands were present that we presumed to be off-target on account of the high reactivity of the maleimide electrophile. HECT E3s were unlikely to be targeted in this experiment because UBE2N lacks the phenylalanine residue at position 63 that is required for HECT binding.^{47–49}

These results illustrate that our ABP may be used to profile endogenous E1–E2 transthiolation activity against a specific E2. We also carried out ABPP of UBA1 in extracted proteomes from a panel of cancer cell lines (Supporting Figure S22). These data suggested transthiolation activity toward UBE2N in certain diseased cells could be deregulated and holds potential as a novel biomarker.

Competitive Activity-based Protein Profiling Further Validates the Mechanism of an E1 Inhibitor. We next carried out experiments to ascertain whether our probe could be used in competitive-ABPP experiments. This has proven to be a powerful strategy for high throughput inhibitor screening, circumventing the requirement for substrate identification and allowing targeted screening against a focused enzymatic step.⁵⁰ We explored two UBA1 inhibitors (Figure 6a). PYR-41 5 inhibits production of E1~Ub *in vitro* and *in vivo* has been proposed to act by covalently modifying the catalytic cysteine of UBA1.⁵¹ However, this is based on the circumstantial evidence that inhibition is lost in the presence of excess small molecule thiol. The second inhibitor was “compound 1” 6, which is pan-specific against human E1s.⁵ Compound 6 forms a covalent adduct with the Ub/Ubl *in situ*, which acts as a nanomolar inhibitor directed against the distinct adenylation activity of E1s (Figure 4b).⁵ We anticipated that this mode of inhibition would not affect labeling with our probe. We initiated UBA1 thioester loading assays with fluorescein-labeled Ub (F-Ub), MgCl₂, and ATP and assessed E1 activity by observing the presence of a ~130 kDa band corresponding to E1~Ub by *in-gel* fluorescence. In control samples, a robust fluorescent signal was observed (Figure 6b, lanes 2 and 3). A control sample was also treated with UBE2N-CN after the formation of E1~Ub. Characteristic of an ABP, UBE2N-CN could act as a covalent mechanism-based inhibitor of UBA1 and even retrospectively

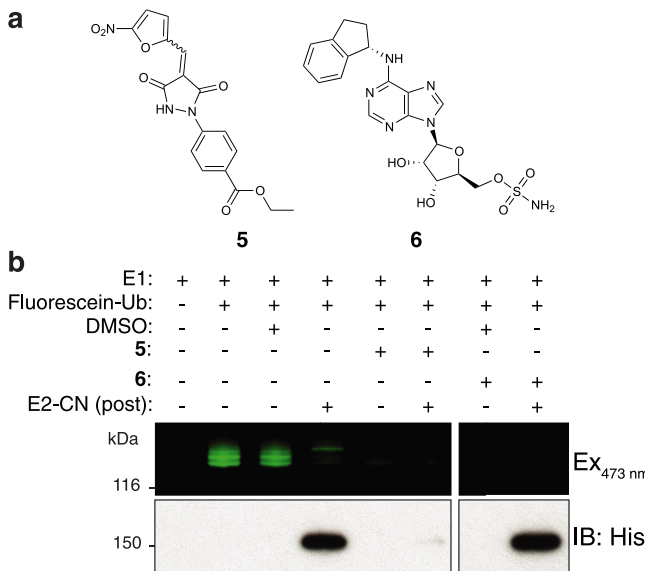


Figure 6. Competitive activity-based protein profiling against UBA1 confirming inhibitor PYR-41 blocks transthiolation. (a) PYR-41 **5** is a covalent inhibitor of UBA1 with an IC₅₀ of <10 μ M. It has been proposed that it covalently modifies C632 in UBA1. “Compound 1” **6** is pan-specific against human E1s and has an IC₅₀ of 5 nM against UBA1.⁵ It targets the adenylation domain of E1s. (b) An in-gel fluorescence-based UBA1 activity assay monitors formation of E1~Ub with fluorescein-labeled Ub (F-Ub). Reaction was initiated by the addition of ATP (2 mM) to UBA1 (500 nM), MgCl₂ (10 mM), and F-Ub (2 μ M). After incubation for 15 min at 37 °C, robust activity is observed in the absence of inhibitor and in the DMSO control (lanes 2 and 3). Post incubation of E1~Ub with His-UBE2-CN (12 μ M) efficiently reverses and inhibits formation of E1~Ub (lane 4). Anti-His immunoblotting (bottom panel) against the His-tag on UBE2N-CN confirms covalent labeling of UBA1 with the probe as evident by the presence of a reactive band at ~150 kDa. Preincubation of UBA1 with **5** (50 μ M) inhibits formation of E1~Ub (lane 5). Covalent probe labeling after post incubation with His-UBE2N-CN is abolished (lane 6, bottom panel). This indicates that **5** does covalently modify C632, rendering it unreactive. This mode of inhibition blocks E1–E2 transthiolation activity. Compound **6** (50 μ M) also inhibits formation of E1~Ub (lane 7). However, labeling with His-UBE2N-CN is completely unaffected. This illustrates the specificity of the His-UBE2N-CN for a distinct step in the E1 catalytic cycle.

deplete E1~Ub as evident by loss of fluorescence signal and a strong signal at ~140 kDa with anti-His immunoblotting, which corresponded to probe-labeled UBA1 (Figure 6b, lane 4). We do not infer that the AVS targets the catalytic cysteine in the context of a thioester linkage, but rather the demonstrated reversibility of E1~Ub formation⁵ (Figure 4a, step 2) continuously regenerates a free catalytic cysteine with which our probe effectively competes. Initial incubation with **5** (50 μ M) efficiently inhibited formation of E1~Ub (Figure 6b, lane 5). Importantly, covalent labeling by post-treatment with UBE2N-CN was completely abolished (Figure 6b, lane 6). This provided further evidence that the catalytic cysteine in UBA1 is rendered unreactive in the presence of **5**, thereby supporting C632 modification as its mode of inhibition. As expected, the addition of **6** (50 μ M) also efficiently inhibited production of E1~Ub, but post-treatment with UBE2N-CN resulted in efficient covalent labeling of UBA1 that was comparable to control samples (Figure 6b, lanes 7 and 8). These results demonstrated that our probe does indeed target a distinct enzymatic step of the E1 activation cycle, and probe

labeling is independent of inhibition of adenylation activity. It also suggests that inhibition of the adenylation activity of E1s does not compromise their ability to recruit E2s which may lead to sequestration of E2s in cells which could account for beneficial or adverse pharmacology, which should warrant further study.

Insight into Transthiolation of RBR E3 Ligases. We next tested whether our probes could label an active RBR E3 ligase. The RBR E3, HOIP, requires activation by complex formation with HOIL-1 or SHARPIN.⁵² However, a recombinant construct consisting of the RBR region is constitutively and highly active and assembles linear Ub chains *in vitro*.⁵² As RBR E3s demonstrate greatest activity with UBE2D and UBE2L3 E2s,¹² we built an acrylonitrile probe on UBE2L3. UBE2L3 contains two noncatalytic cysteine residues (C17 and C137) that we mutated to serine to ensure installation of a single AVS (Supporting Figure S11). This mutant UBE2L3 (UBE2L3*) had comparable activity to wild-type E2 in a linear Ub chain assembly reaction, indicating that E3 binding was not compromised (Supporting Figure S23). We found that HOIP_{RBR} underwent negligible labeling with UBE2L3*-CN even after extended incubation (18 h; Figure 7, lanes 1 and 2).

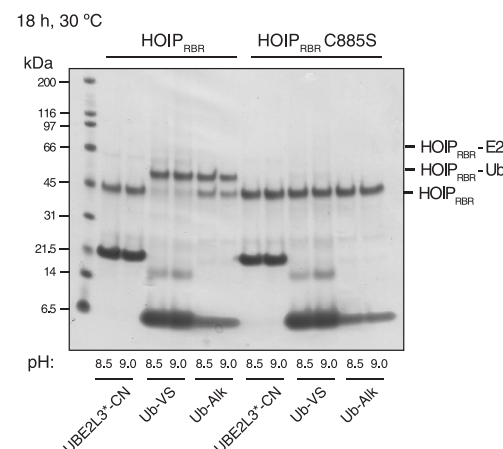


Figure 7. Insight into the determinants of transthiolation activity of an RBR E3 ligase. HOIP_{RBR} and HOIP_{RBR} C885S were incubated with E2- or Ub-based probes. To increase thiol reactivity, incubations were carried out at pH 8.5 and pH 9.0. After 18 h at 30 °C, UBE2L3*-CN did not undergo detectable labeling of HOIP_{RBR} (lanes 1 and 2). However, Ub-VS, bearing a C-terminal vinylsulfone electrophile, and Ub-Alk, bearing a poorly electrophilic alkyne moiety, both specifically labeled HOIP_{RBR} C885 (lanes 3–6). These results suggest that cysteine–cysteine juxtaposition between UBE2L3*-CN and HOIP_{RBR} is not achieved. Efficient labeling with the Ub-based probes indicates Ub is bound by HOIP_{RBR} to position the C-terminus proximal of C885. We propose that a similar binding mode is maintained in the context of E2~Ub whereby the Ub component plays an important mechanistic role in forming a transthiolation-competent complex where cysteine residues are juxtaposed.

The more reactive UBE2L3*-VME probe also failed to label HOIP_{RBR} (data not shown). UBE2L3*-CN was functional as it efficiently labeled E1 (Supporting Figure S12, panel A). This was particularly surprising as probes based on Ub bearing C-terminal warheads have been shown to selectively label the catalytic cysteine residue in other RBR E3s.^{53,54} We next tested whether such Ub probes could modify HOIP_{RBR}. We used ubiquitin-vinylsulfone (Ub-VS) that bears a relatively reactive electrophile, and alkyne-functionalized ubiquitin (Ub-Alk) that

contains an extremely weak electrophile, relative to the acrylonitrile AVS, that can still efficiently label active site cysteines in DUBs by virtue of proximity acceleration.⁵⁵ Remarkably, Ub-VS labeling was near quantitative (Figure 7, lanes 3 and 4) and strictly dependent on C885. Ub-Alk also labeled C885 albeit with reduced efficiency (Figure 7, lanes 5 and 6). These results suggest that labeling with the Ub probes cannot be attributed to hyper-reactivity of the C885 residue alone because, if this were the case, UBE2N-CN would be expected to undergo labeling. Rather, the Ub probe labeling is mediated by a proximity accelerated reaction arising from Ub binding that brings its C-terminus in proximity of C885. This is consistent with a crystal structure of the HOIP RING2 and Ub.⁵⁶ These results suggest that this interaction, or an alternate binding mode, between Ub and RBR is maintained in the context of E2~Ub, whereby the Ub component plays a role in inducing conformation changes in RBR that are required for cysteine–cysteine juxtaposition and therefore transthiolation activity. This has been shown to be the case with HECT E3s where Ub binds the C lobe of the HECT domain, thus bringing the HECT catalytic cysteine in proximity of the E2~Ub thioester bond.⁵⁷ In contrast, complexes between free E2 and HECT have a ~40 Å gap between catalytic cysteines.⁴⁷ On the other hand, the bacterial E3-like effector protein NleL can bind the E2 UBE2L3 and maintain cysteine–cysteine juxtaposition in the absence of Ub.⁵⁸ Consistently, UBE2L3*-VME did label recombinant NleL (Supporting Figure S24). These results suggest Ub itself plays an important role in regulating transthiolation of human E3s. With the bacterial counterparts, at least for NleL, the requirement for Ub is more relaxed.

Herein, we characterized novel biocompatible chemistry that enables the facile installation of proximity-reactive warheads into recombinant proteins. We used this to develop a new class of ABP that targets E1–E2 transthiolation activity, in particular, between UBE2N and UBA1. This enabled target validation of a UBA1 inhibitor, profiling of UBA1 transthiolation activity across a panel of cancer cell lines, and the provision of mechanistic insight into an RBR E3 ligase. This tool provides a platform for profiling UBA1 transthiolation activity in general and could be used to carry out focused competitive-ABPP approaches that specifically target the unexplored pharmacological space associated with E1–E2 transthiolation activity. It should also prove to be valuable for profiling the E1–E2 transthiolation activity in various cellular contexts, thus granting insight into novel disease mechanisms. As UBA1 functions with approximately 35 cognate E2s, activity toward specific E2s might be profiled simply by building ABPs on a recombinant E2 of interest. Furthermore, multiple E1s exist in humans which prime the conjugation of distinct UbIs,⁶ many of whose activities have been implicated with disease.^{15,59} Our NEDD8, SUMO, and ISG15 probes should find utility in studying these systems. Interestingly, when cellular proteomes were treated with ABPs built on UBE2N, the only labeled protein was UBA1. E2s function with E3 ligases, and ~45 of these also undergo transthiolation reactions with E2s. These E3s belong to the HECT and RBR subfamilies. There are several reasons why HECT/RBR E3s were not labeled. Proteomic analyses predict that the cellular abundance of E3s are at least an order of magnitude lower than UBA1,⁶⁰ which could make detection difficult. Furthermore, HECT/RBR E3 ligase activity is often autoinhibited, requiring a cellular stimulus for activation.^{12,61} However, a primary factor might be the absence of ubiquitin, which would normally be covalently attached to the E2

(E2~Ub). Our experiments using an E2 probe in parallel with Ub probes suggest that the ubiquitin component in E2~Ub plays a role in inducing a transthiolation competent conformation in an RBR E3. This mechanism is observed with HECT E3s.^{47,57} To explore this further, second generation probes will be required that incorporate the ubiquitin component. However, we found that our probes did label a pathogenic bacterial HECT E3-like effector. As bacterial E3s have low sequence conservation with their human counterparts, undiscovered E3-like effectors are likely to exist that hold potential as novel drug targets. Our probes should prove to be valuable tools for identifying such effectors.

As the described OTF chemistry described herein labels cysteine residues, cross-orthogonality with other thiol-compatible click reactions such as copper-catalyzed [3 + 2] azide–yne cycloaddition reactions should be a property of OTF allowing development of more sophisticated ABPs and protein-based probes in general. For example, E2 probes could be labeled with fluorescent reporter tags by reaction with genetically encoded unnatural amino acids bearing click handles.⁶² Such fluorescently labeled E2 probes could be used to carry out high throughput screening of potential E1 and E3 inhibitors⁶³ that specifically disrupt E1/E3-E2 interactions.

The OTF chemistry described here may have utility beyond Ub/Ubl conjugating enzymes. Covalent bond formation between proximal cysteines via engineered intermolecular disulfide bonds is a powerful strategy for stabilizing protein complexes but is limited by the redox sensitivity.⁶⁴ The small steric footprint of the heterobisthioether formed using our approach should allow it to be used as a direct, redox-stable substitute for a disulfide bond in certain cases. Furthermore, genetically encoded amino acids bearing electrophilic side chains have recently been used in a powerful methodology known as proximity-enabled protein cross-linking.^{65,66} The strategy described herein draws close parallels with this approach, yet rather than genetic incorporation of a bespoke amino acid, the warhead is installed onto a protein by a simple cysteine labeling reaction. We therefore envision that our OTF approach will be a valuable tool providing a facile entry point into proximity-enabled protein cross-linking experiments. Lastly, OTF could facilitate production of covalent biologics that demonstrate sustained activity over their reversible counterparts.

METHODS

Reaction of GSH (4) with ΔUb-CN and ΔUb-VME (ΔUb-AVS) and Rate Constant Determination. Observed rates, k_{obs} , for the reaction were obtained with a 2000-, 8000- and 16 000-fold excess of reduced GSH in 100 mM Na₂HPO₄, pH 8. GSH solutions of 125 mM, 500 mM, and 1000 mM were then subsequently prepared with a final Na₂HPO₄ concentration of 100 mM (using a stock buffer solution of 1 M Na₂HPO₄, pH 8). ΔUb-AVS solution (60 μM, 100 mM Na₂HPO₄, pH 8) was made up from a stock of ΔUb-CN in MQ water and 1 M Na₂HPO₄, pH 8. The reaction was initiated by the addition of ΔUb-AVS (500 μL, 60 μM) to reduced GSH stock solution (500 μL) in an Eppendorf thermomixer (37 °C, 600 rpm). At defined time points, 100 μL of reaction solution was quenched with 4 μL of quenching solution (25% TFA in acetonitrile) and subjected to LC-MS analysis. Absorbance data at 280 nm were collected for ΔUb-AVS (retention time; ~13.8 min) and the peaks were integrated. Data were fit to an exponential decay function to allow determination of the half-life. The observed rate, k_{obs} , for each run was calculated from the half-life equation:

$$t_{1/2} = \frac{\ln 2}{k_{\text{obs}}}$$

and k_{obs} for each run was plotted against the concentration of reduced GSH to obtain the second order rate constant, k , from the slope of the plot. All data processing was performed using Prism v.6.0d (GraphPad).

Activity-based Labeling of Ub E1 Activating Enzyme with E2 Probes. E2 probes (12 μM) were mixed with E1 enzyme (3 μM) and diluted 10X reaction buffer (500 mM Na₂HPO₄ pH 8) or 10X Ub-ATP buffer (500 mM Na₂HPO₄ pH 8, 20 μM ubiquitin, 20 mM ATP) to a final volume of 15–50 μL . Reactions were incubated at 30 °C and aliquots taken at the specified time points, which were quenched with reducing SDS-gel loading buffer. The quenched reaction solutions were analyzed by reducing SDS-PAGE.

Competitive ABPP of UBA1. Human UBA1 (500 nM) was incubated with 5 (50 μM), 6 (50 μM), or DMSO control in 50 mM Na₂HPO₄, pH 8 buffer for 15 min at RT. Cofactors (Ub-Fluorescein (Boston Biochem U-580), ATP and MgCl₂) were then added as a stock solution (final concentrations of 2 μM , 2 mM, and 10 mM, respectively) to the preincubated samples and were then incubated for a further 15 min at 30 °C. The samples were then divided into two portions and treated with UBE2N-CN, UBE2N-VME, or UBE2N-VME* (12 μM) or buffer (to account for the minor volume change (4%) on E2-probe addition). Samples were then left to incubate for 1 h at 30 °C. 4X SDS loading buffer (nonreducing) was added to a final concentration of 1X. Samples were then subjected to nonreducing 4–12% SDS-PAGE and were analyzed by fluorescence imaging (excitation wavelength 473 nM) on a Fujifilm FLA-1500 imager and by anti-His immunoblotting.

ABPP of Protein Extracts. UBE2N-AVS (5 μM) were added to 125 μg of HEK293 protein extract (50 μL) and incubated at 30 °C for 3 h. Proteins were resolved by SDS-PAGE (10%) and transferred to nitrocellulose. His-tagged species were probed with 1:10 000 anti-His primary antibody (Clontech). Detection was carried out by incubation with 1:2500 antimouse-HRP conjugated antibody (Cell Signaling Technologies) in PBST + 5% milk powder for 1 h at RT. ECL Prime substrate (GE Life Sciences) was used for visualization in accordance with the manufacturers protocol. Probing for UBA1 was carried out with anti-UBA1 primary antibody (Sigma E3152). Detection was carried out by incubation with antimouse-HRP conjugated antibody (Cell Signaling Technologies).

■ ASSOCIATED CONTENT

S Supporting Information

General methods, supporting figures, E2 constructs used, supporting methods, and full MS spectra. This material is available free of charge via the Internet at <http://pubs.acs.org>.

■ AUTHOR INFORMATION

Corresponding Author

*Phone: +44 1382 388738, +44 1223 267 093. Fax: +44 1382 388500. E-mail: s.s.virdee@dundee.ac.uk.

Notes

The authors declare no competing financial interest.

■ ACKNOWLEDGMENTS

We thank P. Cohen and S. Strickson for sharing data and valuable discussion. We are grateful to the MRC-PPU Proteomics Facility, CLS DNA Sequencing Facility, and to N. Wood and M. Wightman of the DNA Cloning Facility. We are also grateful to I. Gilbert for support with chemistry instrumentation. This work was funded by the Scottish Funding Council, the Medical Research Council and pharmaceutical companies supporting the Division of Signal Transduction Therapy (AstraZeneca, Boehringer-Ingelheim, GlaxoSmithKline, Merck KGaA, Janssen Pharmaceutica and Pfizer).

■ REFERENCES

- (1) Popovic, D., Vucic, D., and Dikic, I. (2014) Ubiquitination in disease pathogenesis and treatment. *Nat. Med.* 20, 1242–1253.
- (2) Hershko, A., and Ciechanover, A. (1998) The ubiquitin system. *Annu. Rev. Biochem.* 67, 425–479.
- (3) Curran, M. P., and McKeage, K. (2009) Bortezomib: a review of its use in patients with multiple myeloma. *Drugs* 69, 859–888.
- (4) Van der Veen, A. G., and Ploegh, H. L. (2012) Ubiquitin-like proteins. *Annu. Rev. Biochem.* 81, 323–357.
- (5) Brownell, J. E., Sintchak, M. D., Gavin, J. M., Liao, H., Bruzzese, F. J., Bump, N. J., Soucy, T. A., Milholen, M. A., Yang, X., Burkhardt, A. L., Ma, J., Loke, H.-K., Lingaraj, T., Wu, D., Hamman, K. B., Spelman, J. J., Cullis, C. A., Langston, S. P., Vyskocil, S., Sells, T. B., Mallender, W. D., Visiers, I., Li, P., Claiborne, C. F., Rolfe, M., Bolen, J. B., and Dick, L. R. (2010) Substrate-assisted inhibition of ubiquitin-like protein-activating enzymes: the NEDD8 E1 inhibitor MLN4924 forms a NEDD8-AMP mimetic in situ. *Mol. Cell* 37, 102–111.
- (6) Schulman, B. A., and Harper, J. W. (2009) Ubiquitin-like protein activation by E1 enzymes: the apex for downstream signalling pathways. *Nat. Rev. Mol. Cell Biol.* 10, 319–331.
- (7) Haas, A. L., and Rose, I. A. (1982) The mechanism of ubiquitin activating enzyme. A kinetic and equilibrium analysis. *J. Biol. Chem.* 257, 10329–10337.
- (8) Haas, A. L., Warms, J. V., Hershko, A., and Rose, I. A. (1982) Ubiquitin-activating enzyme. Mechanism and role in protein-ubiquitin conjugation. *J. Biol. Chem.* 257, 2543–2548.
- (9) Hershko, A., Heller, H., Elias, S., and Ciechanover, A. (1983) Components of ubiquitin-protein ligase system. Resolution, affinity purification, and role in protein breakdown. *J. Biol. Chem.* 258, 8206–8214.
- (10) Deshaies, R. J., and Joazeiro, C. A. P. (2009) RING Domain E3 Ubiquitin Ligases. *Annu. Rev. Biochem.* 78, 399–434.
- (11) Kee, Y., and Huibregtse, J. M. (2007) Regulation of catalytic activities of HECT ubiquitin ligases. *Biochem. Biophys. Res. Commun.* 354, 329–333.
- (12) Smit, J. J., and Sixma, T. K. (2014) RBR E3-ligases at work. *EMBO Rep.* 15, 142–154.
- (13) Berndsen, C. E., and Wolberger, C. (2014) New insights into ubiquitin E3 ligase mechanism. *Nat. Struct. Mol. Biol.* 21, 301–307.
- (14) Ye, Y., and Rape, M. (2009) Building ubiquitin chains: E2 enzymes at work. *Nat. Rev. Mol. Cell Biol.* 10, 755–764.
- (15) Bedford, L., Lowe, J., Dick, L. R., Mayer, R. J., and Brownell, J. E. (2011) Ubiquitin-like protein conjugation and the ubiquitin-proteasome system as drug targets. *Nat. Rev. Drug Discovery* 10, 29–46.
- (16) Bossis, G., and Melchior, F. (2006) Regulation of SUMOylation by reversible oxidation of SUMO conjugating enzymes. *Mol. Cell* 21, 349–357.
- (17) Doris, K. S., Rumsby, E. L., and Morgan, B. A. (2012) Oxidative stress responses involve oxidation of a conserved ubiquitin pathway enzyme. *Mol. Cell. Biol.* 32, 4472–4481.
- (18) Tokgöz, Z., Siepmann, T. J., Streich, F., Kumar, B., Klein, J. M., and Haas, A. L. (2012) E1–E2 interactions in ubiquitin and Nedd8 ligation pathways. *J. Biol. Chem.* 287, 311–321.
- (19) Huang, D. T., Miller, D. W., Mathew, R., Cassell, R., Holton, J. M., Roussel, M. F., and Schulman, B. A. (2004) A unique E1–E2 interaction required for optimal conjugation of the ubiquitin-like protein NEDD8. *Nat. Struct. Mol. Biol.* 11, 927–935.
- (20) Olsen, S. K., and Lima, C. D. (2013) Structure of a ubiquitin e1-e2 complex: insights to e1-e2 thioester transfer. *Mol. Cell* 49, 884–896.
- (21) Wang, J., Taherbhoy, A. M., Hunt, H. W., Seyedin, S. N., Miller, D. W., Miller, D. J., Huang, D. T., and Schulman, B. A. (2010) Crystal structure of UBA2(ufd)-Ubc9: insights into E1–E2 interactions in Sumo pathways. *PLoS One* 5, e15805.
- (22) Chatterjee, C., McGinty, R. K., Fierz, B., and Muir, T. W. (2010) Disulfide-directed histone ubiquitylation reveals plasticity in hDot1L activation. *Nat. Chem. Biol.* 6, 267–269.
- (23) Chen, J., Ai, Y., Wang, J., Haracska, L., and Zhuang, Z. (2010) Chemically ubiquitylated PCNA as a probe for eukaryotic translesion DNA synthesis. *Nat. Chem. Biol.* 6, 270–272.

- (24) Tong, H., Hateboer, G., Perrakis, A., Bernardes, R., and Sixma, T. K. (1997) Crystal structure of murine/human Ubc9 provides insight into the variability of the ubiquitin-conjugating system. *J. Biol. Chem.* 272, 21381–21387.
- (25) Chalker, J. M., Bernardes, G. J. L., Lin, Y. A., and Davis, B. G. (2009) Chemical modification of proteins at cysteine: opportunities in chemistry and biology. *Chem. Asian J.* 4, 630–640.
- (26) Spicer, C. D., and Davis, B. G. (2014) Selective chemical protein modification. *Nat. Commun.* 5, 4740.
- (27) Hoogenboom, R. (2010) Thiol-yne chemistry: a powerful tool for creating highly functional materials. *Angew. Chem., Int. Ed. Engl.* 49, 3415–3417.
- (28) Conte, M. L., Staderini, S., Marra, A., Sanchez-Navarro, M., Davis, B. G., and Dondoni, A. (2011) Multi-molecule reaction of serum albumin can occur through thiol-yne coupling. *Chem. Commun. (Cambridge, U. K.)* 47, 11086.
- (29) Li, F., Allahverdi, A., Yang, R., Lua, G. B. J., Zhang, X., Cao, Y., Korolev, N., Nordenskiöld, L., and Liu, C.-F. (2011) A Direct Method for Site-Specific Protein Acetylation. *Angew. Chem., Int. Ed.* 50, 9611–9614.
- (30) Koo, S., Stamenović, M. M., and Prasath, R. A. (2010) Limitations of radical thiol-ene reactions for polymer–polymer conjugation - Koo - 2010 - Journal of Polymer Science Part A: Polymer Chemistry - Wiley Online Library. *J. Polym. Sci., Part A: Polym. Chem.* 48, 1699–1713.
- (31) Grayson, D. H., and O'Donnell, S. H. (2003) Addition of nucleophiles to (E)-3-phenylsulfonylprop-2-enenitrile: a route to β -substituted α , β -unsaturated nitriles and to acetals of cyanoacetaldehyde. *ARKIVOC* 7, 4.
- (32) Strickson, S., Campbell, D. G., Emmerich, C. H., Knebel, A., Plater, L., Ritorto, M. S., Shpiro, N., and Cohen, P. (2013) The anti-inflammatory drug BAY 11–7082 suppresses the MyD88-dependent signalling network by targeting the ubiquitin system. *Biochem. J.* 451, 427–437.
- (33) Shiu, H.-Y., Chan, T.-C., Ho, C.-M., Liu, Y., Wong, M.-K., and Che, C.-M. (2009) Electron-deficient alkynes as cleavable reagents for the modification of cysteine-containing peptides in aqueous medium. *Chemistry* 15, 3839–3850.
- (34) Shiu, H.-Y., Chong, H.-C., Leung, Y.-C., Wong, M.-K., and Che, C.-M. (2010) A highly selective FRET-based fluorescent probe for detection of cysteine and homocysteine. *Chemistry* 16, 3308–3313.
- (35) Truong, V. X., and Dove, A. P. (2013) Organocatalytic, regioselective nucleophilic “click” addition of thiols to propionic acid esters for polymer-polymer coupling. *Angew. Chem., Int. Ed. Engl.* 52, 4132–4136.
- (36) Kuroda, H., Tomita, I., and Endo, T. (1997) A novel phosphine-catalysed polyaddition of terminal acetylenes bearing electron-withdrawing groups with dithiols. Synthesis of polymers having dithioacetal moieties in the main chain. *Polymer* 38, 6049–6054.
- (37) Komander, D., Clague, M. J., and Urbé, S. (2009) Breaking the chains: structure and function of the deubiquitinases. *Nat. Rev. Mol. Cell Biol.* 10, 550–563.
- (38) Borodovsky, A., Ovaa, H., Kolli, N., Gan-Erdene, T., Wilkinson, K. D., Ploegh, H. L., and Kessler, B. M. (2002) Chemistry-based functional proteomics reveals novel members of the deubiquitinating enzyme family. *Chem. Biol.* 9, 1149–1159.
- (39) Katrun, P., and Chiampanichayakul, S. (2010) PhI(OAc)₂/KI-Mediated Reaction of Aryl Sulfonates with Alkenes, Alkynes, and $\alpha\beta$ -Unsaturated Carbonyl Compounds: Synthesis of Vinyl Sulfones and β -Iodovinyl Sulfone. *Eur. J. Org. Chem.* 2010, 5633–5641.
- (40) Serafimova, I. M., Pufall, M. A., Krishnan, S., Duda, K., Cohen, M. S., Maglathlin, R. L., McFarland, J. M., Miller, R. M., Frödin, M., and Taunton, J. (2012) Reversible targeting of noncatalytic cysteines with chemically tuned electrophiles. *Nat. Chem. Biol.* 8, 471–476.
- (41) Skaug, B., Jiang, X., and Chen, Z. J. (2009) The role of ubiquitin in NF-kappaB regulatory pathways. *Annu. Rev. Biochem.* 78, 769–796.
- (42) Panier, S., and Durocher, D. (2009) Regulatory ubiquitylation in response to DNA double-strand breaks. *DNA Repair (Amst.)* 8, 436–443.
- (43) Chen, J. J., Tsu, C. A., Gavin, J. M., Milhollen, M. A., Bruzzese, F. J., Mallender, W. D., Sintchak, M. D., Bump, N. J., Yang, X., Ma, J., Loke, H.-K., Xu, Q., Li, P., Bence, N. F., Brownell, J. E., and Dick, L. R. (2011) Mechanistic studies of substrate-assisted inhibition of ubiquitin-activating enzyme by adenosine sulfamate analogues. *J. Biol. Chem.* 286, 40867–40877.
- (44) Pickart, C. M., Kasperek, E. M., Beal, R., and Kim, A. (1994) Substrate properties of site-specific mutant ubiquitin protein (G76A) reveal unexpected mechanistic features of ubiquitin-activating enzyme (E1). *J. Biol. Chem.* 269, 7115–7123.
- (45) Smith, M. E. B., Schumacher, F. F., Ryan, C. P., Tedaldi, L. M., Papaioannou, D., Waksman, G., Caddick, S., and Baker, J. R. (2010) Protein Modification, Bioconjugation, and Disulfide Bridging Using Bromomaleimides. *J. Am. Chem. Soc.* 132, 1960–1965.
- (46) Gorin, G., Martic, P. A., and Doughty, G. (1966) Kinetics of the reaction of N-ethylmaleimide with cysteine and some congeners. *Arch. Bichem. Biophys.* 115, 593–597.
- (47) Huang, L., Kinnucan, E., Wang, G., Beaudenon, S., Howley, P. M., Huibregtse, J. M., and Pavletich, N. P. (1999) Structure of an E6AP-UbcH7 complex: insights into ubiquitination by the E2-E3 enzyme cascade. *Science* 286, 1321–1326.
- (48) Nuber, U., and Scheffner, M. (1999) Identification of determinants in E2 ubiquitin-conjugating enzymes required for hec E3 ubiquitin-protein ligase interaction. *J. Biol. Chem.* 274, 7576–7582.
- (49) Eletr, Z. M., and Kuhlman, B. (2007) Sequence determinants of E2-E6AP binding affinity and specificity. *J. Mol. Biol.* 369, 419–428.
- (50) Niphakis, M. J., and Cravatt, B. F. (2014) Enzyme inhibitor discovery by activity-based protein profiling. *Annu. Rev. Biochem.* 83, 341–377.
- (51) Yang, Y., Kitagaki, J., Dai, R.-M., Tsai, Y. C., Lorick, K. L., Ludwig, R. L., Pierre, S. A., Jensen, J. P., Davydov, I. V., Oberoi, P., Li, C.-C. H., Kenten, J. H., Beutler, J. A., Vousden, K. H., and Weissman, A. M. (2007) Inhibitors of ubiquitin-activating enzyme (E1), a new class of potential cancer therapeutics. *Cancer Res.* 67, 9472–9481.
- (52) Stieglitz, B., Morris-Davies, A. C., Koliopoulos, M. G., Christodoulou, E., and Rittinger, K. (2012) LUBAC synthesizes linear ubiquitin chains via a thioester intermediate. *EMBO Rep.* 13, 840–846.
- (53) Wauer, T., and Komander, D. (2013) Structure of the human Parkin ligase domain in an autoinhibited state. *EMBO J.* 32, 2099–2112.
- (54) Park, S., Krist, D. T., and Statsyuk, A. V. (2015) Protein ubiquitination and formation of polyubiquitin chains without ATP, E1 and E2 enzymes. *Chem. Sci.* 6, 1770–1779.
- (55) Ekkebus, R., van Kasteren, S. I., Kulathu, Y., Scholten, A., Berlin, I., Geurink, P. P., de Jong, A., Goerdalay, S., Neefjes, J., Heck, A. J. R., Komander, D., and Ovaa, H. (2013) On terminal alkynes that can react with active-site cysteine nucleophiles in proteases. *J. Am. Chem. Soc.* 135, 2867–2870.
- (56) Stieglitz, B., Rana, R. R., Koliopoulos, M. G., Morris-Davies, A. C., Schaeffer, V., Christodoulou, E., Howell, S., Brown, N. R., Dikic, I., and Rittinger, K. (2013) Structural basis for ligase-specific conjugation of linear ubiquitin chains by HOIP. *Nature* 503, 422–426.
- (57) Kamadurai, H. B., Souphron, J., Scott, D. C., Duda, D. M., Miller, D. J., Stringer, D., Piper, R. C., and Schulman, B. A. (2009) Insights into ubiquitin transfer cascades from a structure of a UbcHSB approximately ubiquitin-HECT(NEDD4L) complex. *Mol. Cell* 36, 1095–1102.
- (58) Lin, D. Y.-W., Diao, J., and Chen, J. (2012) Crystal structures of two bacterial HECT-like E3 ligases in complex with a human E2 reveal atomic details of pathogen-host interactions. *Proc. Natl. Acad. Sci. U. S. A.* 109, 1925–1930.
- (59) Kessler, J. D., Kahle, K. T., Sun, T., Meerbrey, K. L., Schlabbach, M. R., Schmitt, E. M., Skinner, S. O., Xu, Q., Li, M. Z., Hartman, Z. C., Rao, M., Yu, P., Dominguez-Vidana, R., Liang, A. C., Solimini, N. L., Bernardi, R. J., Yu, B., Hsu, T., Golding, I., Luo, J., Osborne, C. K., Creighton, C. J., Hilsenbeck, S. G., Schiff, R., Shaw, C. A., Elledge, S. J., and Westbrook, T. F. (2012) A SUMOylation-dependent transcriptional subprogram is required for Myc-driven tumorigenesis. *Science* 335, 348–353.

- (60) Geiger, T., Wehner, A., Schaab, C., Cox, J., and Mann, M. (2012) Comparative proteomic analysis of eleven common cell lines reveals ubiquitous but varying expression of most proteins. *Mol. Cell Proteomics* **11**, M111.014050.
- (61) Wiesner, S., Ogunjimi, A. A., Wang, H.-R., Rotin, D., Sicheri, F., Wrana, J. L., and Forman-Kay, J. D. (2007) Autoinhibition of the HECT-type ubiquitin ligase Smurf2 through its C2 domain. *Cell* **130**, 651–662.
- (62) Nguyen, D. P., Lusic, H., Neumann, H., Kapadnis, P. B., Deiters, A., and Chin, J. W. (2009) Genetic encoding and labeling of aliphatic azides and alkynes in recombinant proteins via a pyrrolysyl-tRNA Synthetase/tRNA(CUA) pair and click chemistry. *J. Am. Chem. Soc.* **131**, 8720–8721.
- (63) Bachovchin, D. A., Brown, S. J., Rosen, H., and Cravatt, B. F. (2009) Identification of selective inhibitors of uncharacterized enzymes by high-throughput screening with fluorescent activity-based probes. *Nat. Biotechnol.* **27**, 387–394.
- (64) Heikoop, J. C., van den Boogaart, P., Mulders, J. W., and Grootenhuis, P. D. (1997) Structure-based design and protein engineering of intersubunit disulfide bonds in gonadotropins. *Nat. Biotechnol.* **15**, 658–662.
- (65) Xiang, Z., Ren, H., Hu, Y. S., Coin, I., Wei, J., Cang, H., and Wang, L. (2013) Adding an unnatural covalent bond to proteins through proximity-enhanced bioreactivity. *Nat. Methods* **10**, 885–888.
- (66) Coin, I., Katritch, V., Sun, T., Xiang, Z., Siu, F. Y., Beyermann, M., Stevens, R. C., and Wang, L. (2013) Genetically encoded chemical probes in cells reveal the binding path of urocortin-I to CRF class B GPCR. *Cell* **155**, 1258–1269.

■ NOTE ADDED AFTER ASAP PUBLICATION

This paper originally posted April 15, 2015. Revisions to Figures 3 and 4 and the Supporting Information file have been made and the paper was re-posted April 20, 2015.